

Use of *Cynara scolymus* as Green Corrosion Inhibitor for Carbon Steel in Sulfuric Acid

M. G. Valladares-Cisneros¹, A. Esquivel-Rojas², V.M. Salinas-Bravo³, J. G. Gonzalez-Rodríguez²

¹ Universidad Autónoma del Estado de Morelos, Facultad de Ciencias Químicas e Ingeniería., Ave. Universidad 1001, Chamilpa, C.P. 62209, Cuernavaca, Mor. Mexico.

² Universidad Autónoma del Estado de Morelos, Centro de Investigaciones en Ingeniería y Ciencias Aplicadas, Ave. Universidad 1001, Chamilpa, C.P. 62209, Cuernavaca, Mor. Mexico.

³ Instituto de Investigaciones Electricas. Gerencia de Materiales y Procesos Químicos, Av. Reforma 113. Cuernavaca. Morelos. 062000. Mexico.

*E-mail: ggonzalez@uaem.mx

Received: 29 April 2016 / Accepted: 25 June 2016 / Published: 7 August 2016

A study on the use of *Cynara scolymus* (*C. scolymus*) as a green corrosion inhibitor for 1018 carbon steel in 0.5 M sulfuric acid has been carried out by using weight loss tests, potentiodynamic polarization curves and electrochemical impedance spectroscopy measurements. It was found that *C. scolymus* is a good corrosion inhibitor with its efficiency increasing with the inhibitor concentration but it decreases with an increase in the temperature. *C. scolymus* is a mixed type of inhibitor, which is physically adsorbed on to the metal surface by following a Temkin adsorption isotherm. It forms a protective film by the contained compounds such as fatty acids, phenolics as quinic acid and sterols such as stigmaterol and γ -sitosterol .

Keywords: Carbon steel, acid corrosion, green inhibitor.

1. INTRODUCTION

The amount of sulphuric acid used in the chemical industry for removal of the undesired scales and rust is enormous. In order to secure the metal against the acid attack, is a common practice the addition of corrosion inhibitors, and a lot of research in this regard have been carried out using organic inhibitors [1-4]. Commonly used inhibitors are organic compounds which contain hetero-atoms such as N, S and O, which have a high electron density that makes them the reaction centres. The way that these compounds retard corrosion attack is being adsorbed on the metallic surface and block the active corrosion sites, but unfortunately most of them are highly toxic to both human beings and environment

[5-7]. Thus, it is necessary to use compounds which are compatible with environment, cheaper and harmless as corrosion inhibitors [8-23]. This kind of inhibitors has been used as extract or oil and may play a major role in protecting metals from attack in pickling and/or bath acid solutions. Thus, Khan et al. [15] carried out a review of the literature that reports the use of green corrosion inhibitors and found that those compounds which have N, S or O in their molecular structure showed excellent corrosion inhibition properties. Anupama [18] evaluated the use of *Pimenta dioica* as corrosion inhibitor for mild steel in HCl by using electrochemical techniques and weight loss measurements. In addition, they used computational calculations for the molecular components to study the corrosion inhibition mechanism. Ji et al. [19] used *Musa paradisiaca* (Banana) peels as corrosion inhibitor for mild steel in HCl finding a good corrosion inhibition, but raw banana peels extract had a better efficiency than that for the ripe ones. Ngobiri evaluated *Brassica oleracea* as a green inhibitor for pipeline steel in 0.5M H₂SO₄ [20]. They found that the corrosion inhibition efficiency increased with the inhibitor concentration and temperature up to a point, but decreased with a further increase in either the concentration or the temperature. Similar studies were performed with mild steel in HCl by using extracts of *Retama monosperma* [21], *Eleusine aegyptiaca* and *Croton rottleri leaf* [22].

Artichoke or *Cynara scolymus* L. (*C. scolymus*) is an old plant, which comes from Mediterranean sea, Italy and Spain. Its parts, such as leaves, have been enjoyed as a vegetable all over the world and are used in herbal medicine as a choleric from a long time [23]. Polyphenols and flavonoids have been found as a fundamental part in the chemical components of artichoke leaves but some mono- and dicaffeoylquinic acids have been reported [24-25]. Not only some antibacterial and anti oxidative properties have been reported in various pharmacological tests done to artichoke leaf extracts but also some anti-HIV, bile expelling, hepatoprotective, urinate, and choleric activities as the ability to inhibit cholesterol biosynthesis and LDL oxidation [26-28]. Working with cultured rat hepatocytes, leaf extracts have been reported to show anti oxidative and protective properties against hydroperoxide-induced oxidative stress [29], as well as certain ability to protect lipoprotein from oxidation in vitro [30], haemolysis induced by hydrogen peroxide, to inhibit oxidative stress when human cells are stimulated with agents that generate hydrogen peroxide, phorbol-12-myristate-13-acetate, and *N*-formyl-methionyl-leucyl-phenylalanine [31]. Thus, the goal of this research work is to evaluate artichoke petals extract (*C. scolymus*) as corrosion inhibitor for carbon steel in acid media.

2. EXPERIMENTAL PROCEDURE.

2.1 Testing Solution

Commercial *C. scolymus* was purchased from a local market, and left to dry in air. After two weeks, the petals were removed and soaked into methanol during 72 hours, after which the remaining methanol was evaporated completely. A paste was obtained this way which was used to be dissolved in methanol as stock solution. Concentrations used in this work include 0, 100, 200, 400, 600, 800 and

1000 ppm. As corrosive environment, a 0.5 M H₂SO₄ solution was prepared by using analytical grade reagents.

2.2 Material tested.

As testing material, a 6.0 mm diameter 1018 carbon steel rod was used. For electrochemical tests, a 2.0 cm long specimen was encapsulated in commercial polymeric resin, abraded with 600 grade SiC emery paper, washed and degreased with acetone and used.

2.3 Electrochemical techniques.

Electrochemical techniques used in this work includes potentiodynamic polarization curves and electrochemical impedance spectroscopy (EIS) measurements. A conventional three electrodes glass cell was used, with an Ag/AgCl and a graphite rod as reference and auxiliary electrodes respectively. For the polarization curves, electrodes were let to reach a steady state free corrosion potential value, E_{corr}, normally during 30 minutes. After this, specimen was polarized from -1500 to +2000 mV respect to the E_{corr} value, at a scan rate of 1 mV/s. For the EIS measurements, specimens were applied a signal with an amplitude of ± 10 mV around the E_{corr} value in a frequency interval of 10 kHz-0.05 Hz.

2.4 Weight loss tests.

Cylindrical coupons measuring 2.5 cm high and 6.0 mm of diameter were cut; they were abraded with 600 grade emery paper, rinsed in distilled water, dried with warm air, degreased with acetone dried and finally kept in a desiccator before their use. Then they were immersed into the 0.5 M H₂SO₄ aggressive solution and used different concentrations of green inhibitor of *C. scolymus* (0 - 1000 ppm) during 72 h. Testing temperatures included 25°C, 40 and 60°C. All tests were done for triplicated. Corrosion rates, in terms of weight loss measurements, ΔW, were calculated as follows:

$$\Delta W = (m_1 - m_2) / A \quad (1)$$

In eq. (1) the mass of the specimen before and after corrosion tests are m_1 m_2 respectively, and the exposed area of the specimen is A . Inhibitor efficiency, IE , was calculated as follows:

$$IE (\%) = 100 (\Delta W_1 - \Delta W_2) / \Delta W_1 \quad (2)$$

with ΔW₁ and ΔW₂ as the weight loss without and with inhibitor respectively. Selected specimens were observed in a LEO 1450VP scanning electron microscope (SEM) for their analysis.

2.5 FTIR Spectroscopic analysis of green corrosion inhibitor

The green corrosion inhibitor was examined under FTIR analysis by using a Bruker equipment in KBr pellet in the 4500-570 cm⁻¹ interval. The peak values of the FTIR were recorded. Each analysis was repeated twice to detect the characteristic peaks and their functional groups.

2.6 Gas Chromatography / Mass spectrometry (GC-MS) analysis

The *C. scolymus* green corrosion inhibitor was also analyzed on an GC Agilent 6890 System Plus coupled to Agilent 5973 Network Mass selective detector, to detect all majority organic natural compounds content in the methanol extract. The GC-MS equipped with silica capillary column (30 m X 0.25 mm, film thickness 0.25mm). The GC conditions were temperature 45 to 250 °C with a temperature gradient of 10 °C/min. Injected a volume 1.0 µL of green corrosion inhibitor at 0.02 g/L of concentration. The identification of the majority of components was based on the comparison of their indices mass fragmentation with those of authentic compounds on the commercial equipment high quality mass spectra database N-15598 [32, 33].

3. RESULTS AND DISCUSSION

3.1 Weight loss tests

Table 1. Effect of *C. scolymus* concentration on the weight loss, inhibitor efficiency and surface coverage degree for 1018 carbon steel in 0.5 M H₂SO₄ at different temperatures.

C _{inh} (ppm)		Δ W (mg/cm ²)	I.E. (%)	Θ
25 °C	0	125	—	—
	100	98	22	0.22
	200	83	34	0.34
	400	45	64	0.64
	600	31	75	0.75
	800	20	84	0.84
	1000	14	89	0.89
	40 °C	0	235	—
100		210	12	0.12
200		190	19	0.19
400		145	38	0.38
600		122	48	0.48
800		85	63	0.63
1000		55	76	0.76
60 °C		0	250	—
	100	220	9	0.09
	200	210	15	0.15
	400	160	35	0.35
	600	137	45	0.45
	800	95	60	0.60
	1000	61	70	0.70

The effect of *C. scolymus* concentration on the weight loss, inhibitor efficiency and surface coverage area, Θ , is given in table 1, where it can be seen the clear effect of this green inhibitor in the weight loss, which decreases with increasing the inhibitor concentration, while the inhibitor efficiency and Θ value increases. It is clear that the increase in the inhibitor efficiency values is due to an increase in the surface covered by the inhibitor, as indicated by an increase in the Θ value. It can be seen that the weight loss increases whereas the inhibitor efficiency decreases with increasing the temperature.

To investigate the adsorption behaviour of *C. scolymus* extract in H_2SO_4 solution, several isotherm models were employed, but, as shown in Fig. 1, the best fit was obtained by using the Temkin type of isotherm at the three testing temperatures.

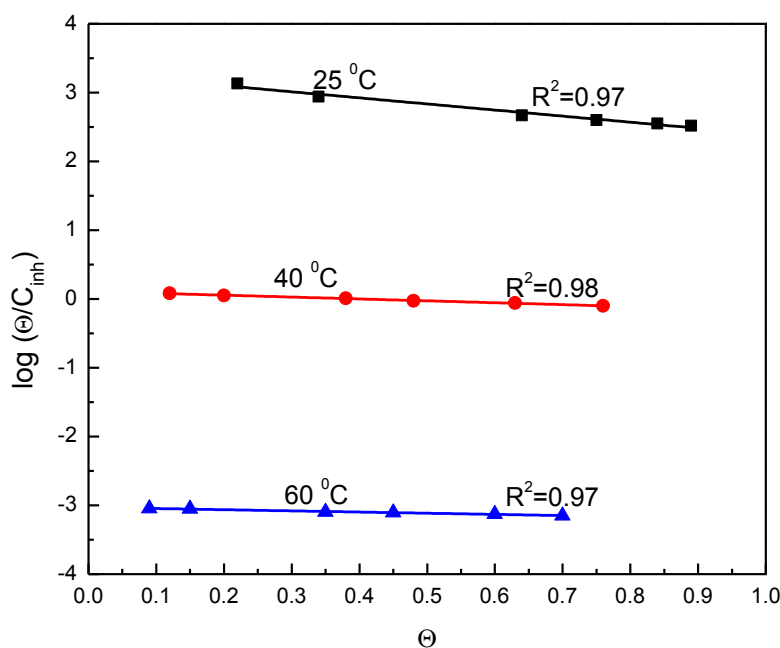


Figure 1. Temkin type of adsorption isotherm for 1018 carbon steel in in 0.5 M H_2SO_4 containing *C. scolymus* at 25, 40 and 60 °C.

This isotherm model monitors the variation of adsorption coefficient K_{ads} with concentration of inhibitor, C_{inh} , according to the following relationship [34]:

$$\log(\theta/C_{inh}) = \log(K_{ads}) - A\theta \tag{3}$$

where A is a constant. From the Temkin isotherm, the adsorption-desorption equilibrium constant K_{ads} was determined as 8.57, 0.13 and 0.0014 $L\ mg^{-1}$ at 25, 40 and 60 °C respectively, indicating. This leads to an adsorption free-energy value of -17.4 , -1.3 and 12.5 $kJ\ mol^{-1}$ at 25, 40 and 60 °C respectively. The K_{ads} value may be taken as a measure of the strength of the adsorption forces between the inhibitor molecules and the metal surface [35]. Large values of K_{ads} imply more efficient

adsorption and hence better inhibition efficiency [36]. Generally, values of the adsorption free-energy around -20 kJ mol^{-1} have typically been correlated with the electrostatic interactions between organic molecules and charged metal surface (physisorption) whilst those values in the order of -40 kJ mol^{-1} are associated with charge sharing or transfer from the organic molecules to the metal surface (chemisorption) to form a co-ordinate type of bond [37]. The negative value of the free-energy of adsorption value means that the adsorption process is spontaneous, while the value around -20 kJ mol^{-1} indicates that *C. scolymus* was physically adsorbed on the steel surface.

3.2 Polarization curves.

The effect of *C. scolymus* concentration in the polarization curves for 1018 carbon steel in 0.5 M H_2SO_4 is given in Fig. 2- This figure shows that steel display an active-passive behavior regardless of the inhibitor concentration. The E_{corr} value shifted towards more active values as soon as *C. scolymus* was added to the system, except with the addition of 1000 ppm, where it moved towards a more active value. The corrosion and passive current density values were lowered when *C. scolymus* was added for almost one order of magnitude, reaching its lowest value with 1000 ppm. Electrochemical parameters obtained from these polarization curves are shown in table 2, where it can be seen that anodic Tafel slope was increased when the inhibitor was added, except when 1000 ppm were added and where the highest inhibitor efficiency was obtained and where the anodic Tafel slope was decreased.

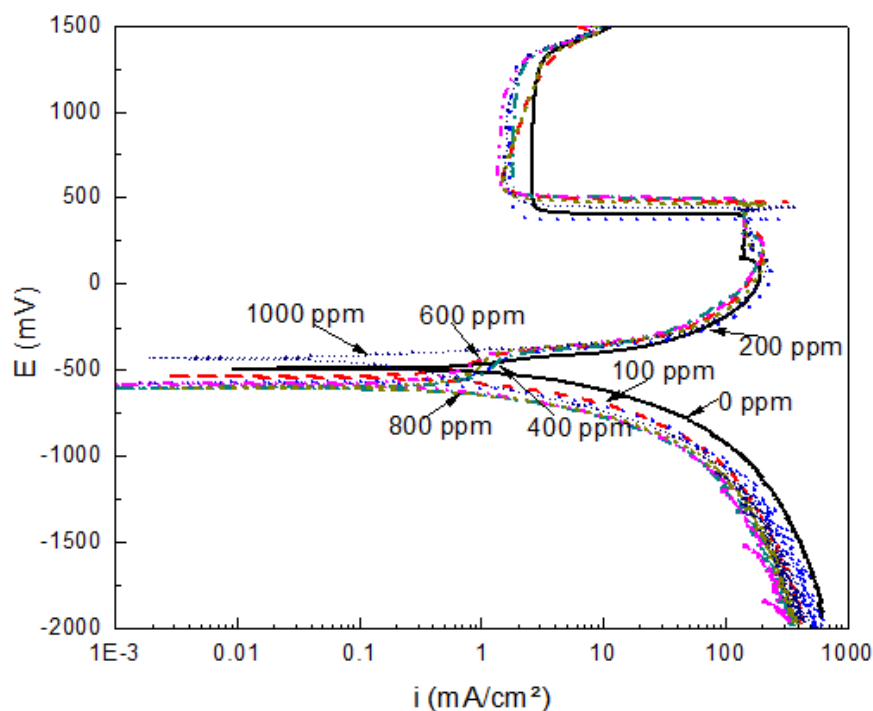


Figure 2. Effect of *C. scolymus* concentration in the polarization curves for 1018 carbon steel in in 0.5 M H_2SO_4 .

On the other hand, cathodic Tafel slope was decreased when the inhibitor was added, except when 1000 ppm were added, where it was increased. Thus, *C. scolymus* is a type of mixed inhibitor for carbon steel in 0.5 M H₂SO₄, decreasing both the anodic dissolution of iron and cathodic hydrogen evolution reactions.

Table 2. Electrochemical parameters obtained from the polarization curves for 1018 carbon steel in 0.5 M H₂SO₄.

C _{inh} (ppm)	E _{corr} (mV)	I _{corr} (mA cm ⁻²)	I _{pas} (mA cm ⁻²)	β _a (mV/Dec)	β _c (mV/Dec)	I.E. (%)	Θ
0	-490	1.185	2.7	80	120		
100	-539	0.721	2.0	200	100	38	0.38
200	-570	0.551	1.8	365	115	53	0.53
400	-605	0.535	1.6	275	125	57	0.57
600	-580	0.452	1.5	265	110	61	0.61
800	-605	0.409	1.4	500	105	66	0.66
1000	-430	0.1464	1.2	42	155	88	0.88

3.3 Electrochemical impedance spectroscopy measurements.

EIS data, in both Nyquist and Bode formats for 1018 carbon steel in 0.5 M H₂SO₄ at different concentrations of *C. scolymus* are given in Fig. 3. Nyquist diagrams, Fig. 3 a, display a single depressed, capacitive-like semicircle with its center in the real axis, with a tale or elongations at low frequency values, which is due to the accumulation of all kind of species at the metal/solution interface [38, 39].

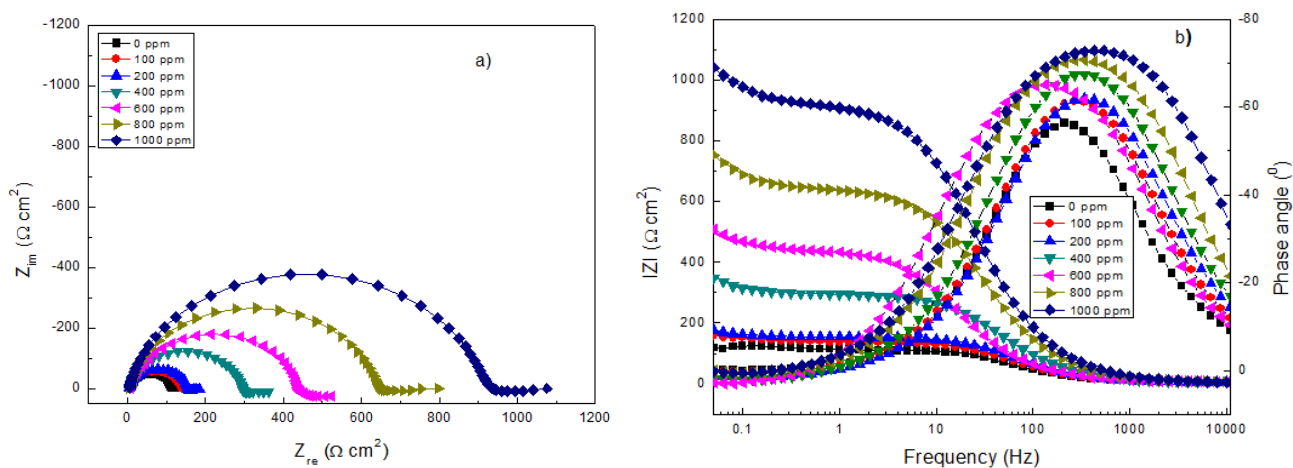


Figure 3. Effect of *C. scolymus* concentration in the a) Nyquist and b) Bode plots for 1018 carbon steel in in 0.5 M H₂SO₄.

When Nyquist data display only a single semicircle, this means an activation control, i.e. the corrosion process is under charge transfer control from the metal to the electrolyte through the double electrochemical layer. The semicircle diameter increases with increasing *C. scolymus* concentration.

On the other hand, Bode plots, Fig. 3 b, shows that the impedance modulus increases as the *C. scolymus* increases, and the presence of a single in the uninhibited solution. As the *C. scolymus* concentration increases, this peak shifts towards higher frequency values and the frequency interval where the phase angle remains constant increases, indicating that the corrosion protection given by *C. scolymus* increases. The frequency interval where the phase angle remained constant was with the addition of 1000 ppm of *C. scolymus*, indicating that the highest corrosion resistance was obtained at this inhibitor concentration.

Table 3. Electrochemical parameters obtained from the EIS data for 1018 carbon steel in 0.5 M H₂SO₄.

C _{inh} (ppm)	R _s (Ω cm ²)	R _{tc} (Ω cm ²)	C _{dl} (F cm ⁻²)	I.E. (%)	Θ
0	6	106	3.8X10 ⁻⁵	----	----
100	5	135	2.9X10 ⁻⁵	22	0.27
200	6	159	2.0X10 ⁻⁵	34	0.39
400	5	293	1.7X10 ⁻⁵	64	0.69
600	7	431	3.0X10 ⁻⁵	75	0.78
800	6	641	1.2X10 ⁻⁵	84	0.84
1000	5	930	1.1X10 ⁻⁵	89	0.90

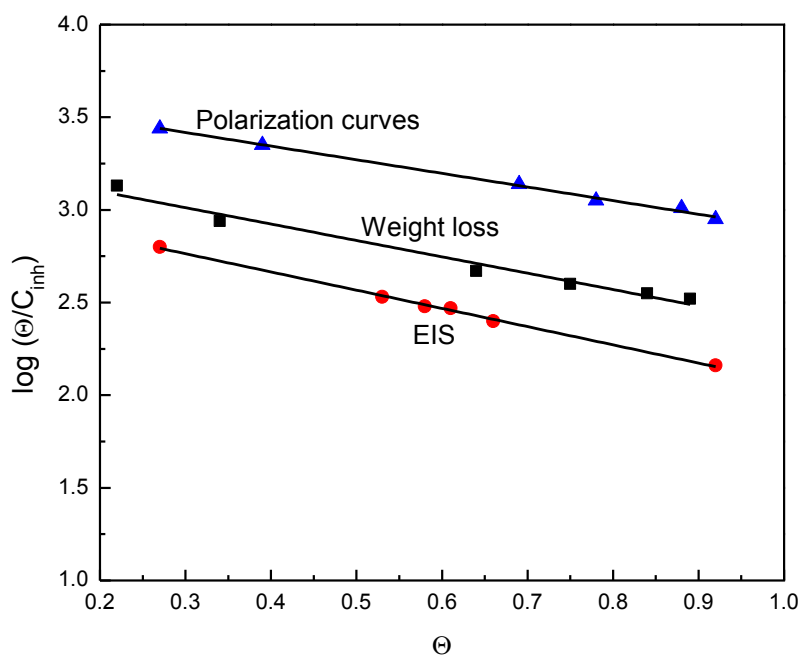


Figure 4. Temkin type of adsorption isotherm for 1018 carbon steel in in 0.5 M H₂SO₄ containing *C. scolymus* using weight loss, polarization curves anad EIS data at 25 °C.

The increase in the impedance with increasing the inhibitor concentration is due to the adsorption of the inhibitor on the surface metal and an increase in the surface area covered by the inhibitor molecules, as it can be seen in table 3, where the electrochemical parameters obtained from EIS data are given. In this table, R_s is the solution resistance, R_{ct} the charge transfer resistance, and C_{dl} the double layer capacitance. Inhibitor efficiency was calculated with following equation:

$$I.E. (\%) = 100 (R_{ct1} - R_{ct2}) / R_{ct1} \quad (4)$$

where R_{ct1} is the charge transfer resistance with inhibitor and R_{ct2} the charge transfer resistance without inhibitor. It can be seen that the R_{ct} value increases with the inhibitor concentration, decreasing, thus, the corrosion rate, reaching a highest value when 1000 ppm of inhibitor are added. On the other hand, the C_{dl} value decreases with an increase in the inhibitor concentration, reaching its lowest value with the addition of 1000 ppm. An increase in R_{ct} indicates a higher metal surface area covered by the inhibitor as a result of an increase in inhibitor concentration [35, 36] which avoid the electrolyte molecules to attack the metal. Adsorption isotherms can be calculated by using both, gravimetric and electrochemical data, which is given in Fig. 4, which shows that the same adsorption isotherm was obtained, i. e. Temkin, with the three different techniques, which is very encouraging. The values of the double-layer capacitance (C_{dl}) decrease by adding inhibitor in to corrosive solution. A different method to calculate double-layer capacitance is by using following equation:

$$C_{dl} = \epsilon \epsilon_0 A / \delta \quad (5)$$

where ϵ is the double layer dielectric constant, ϵ_0 the vacuum electrical permittivity, δ the double layer thickness, and A the surface area. Thus, if the water molecules are replaced by the inhibitor molecules being adsorbed, which have lower dielectric constant [37], this will decrease the double layer thickness and, consequently, a decrease in C_{dl} value.

3.4 SEM micrographs.

Some surface SEM micrographs of specimens corroded without and with 1000 ppm of *C. scolymus* at 25, 40 and 60 °C can be seen in Fig. 5.

For the blank, uninhibited solution, micrographs show a corrosion products film with many porous and cracks, which increase in number as the testing temperature increases, Fig. 5 a, c and e; these cracks which are paths for the corrosive solution to ingress and attack the underlying metal. For the solution containing 1000 ppm of *C. scolymus*, micrographs show a corrosion products film with much less amount of porous and cracks, especially at 25 °C, Fig. 5 b, which is an indication that this film is the responsible for the corrosion protection given by the inhibitor.

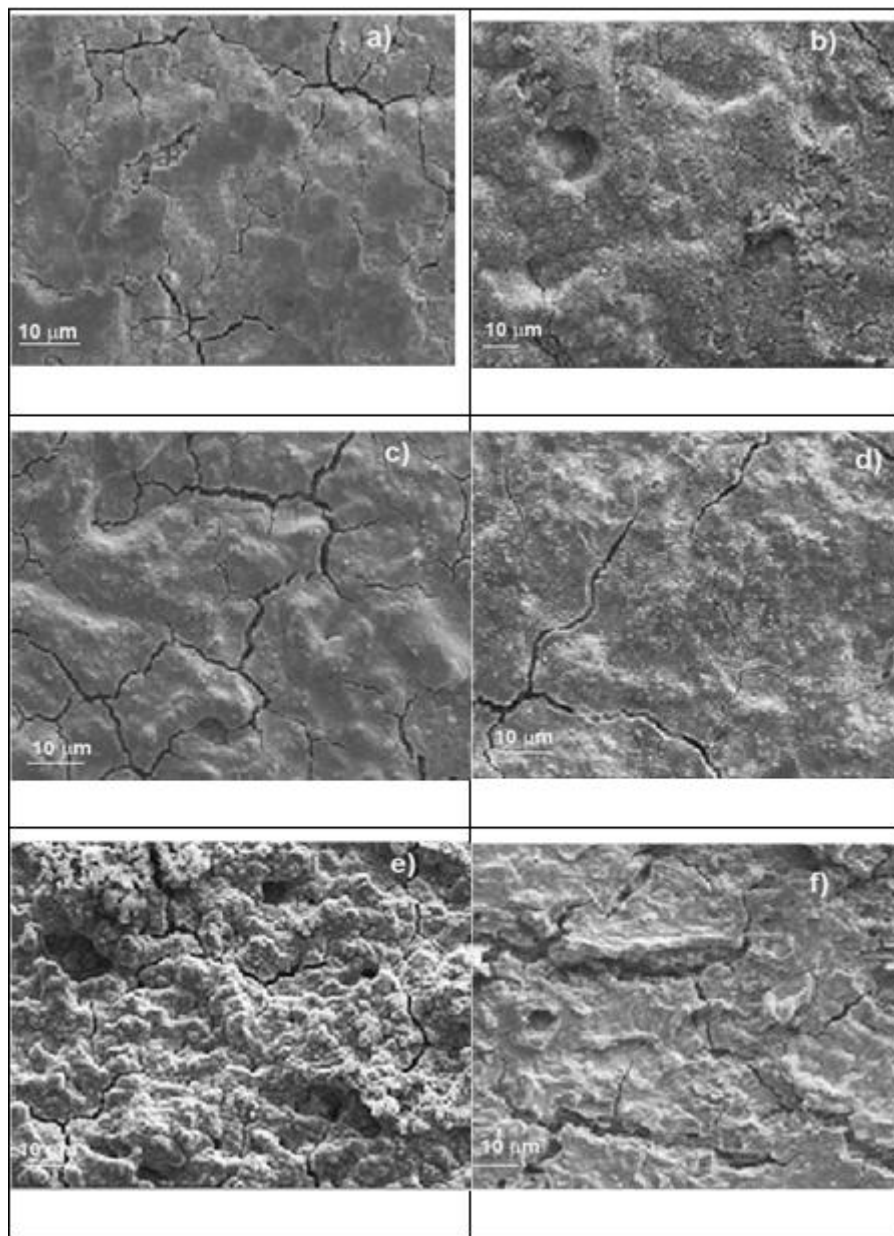
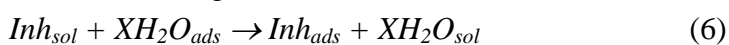
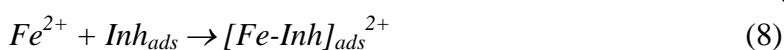


Figure 5. SEM micrographs of 1018 carbon steel corroded in 0.5 M H₂SO₄ containing 0 ppm (a, c and e) and 1000 ppm (b, d and f) of *C. scolymus* at 20 (a and b), 40 (c and d) and 60 °C (e and f).

As the temperature increases, Fig. 5 d and f, the amount of cracks present in the film increases, decreasing, thus, the corrosion protection given by the film. This film is formed by the reaction of iron ions and inhibitor, which replaces the water molecules from the metal surface is adsorbed onto the metal surface, according to:



C. scolymus may then react with iron ions, Fe^{2+} , generated during its corrosion to form a complex [40, 41]:



which is the responsible for the corrosion protection given to the metals surface.

3.6 Infrared Spectroscopy.

FTIR spectrum for *C. scolymus* extract is shown in Fig.6, where a typical signal of the O-H link, which is known to passivate metals, can be seen at 3382 cm^{-1} , and another one at 2931 cm^{-1} corresponds to the C-H signal, whereas a strong signal at 2361 cm^{-1} is for the C-O link, which is an evidence of the presence of the carboxylic acid.

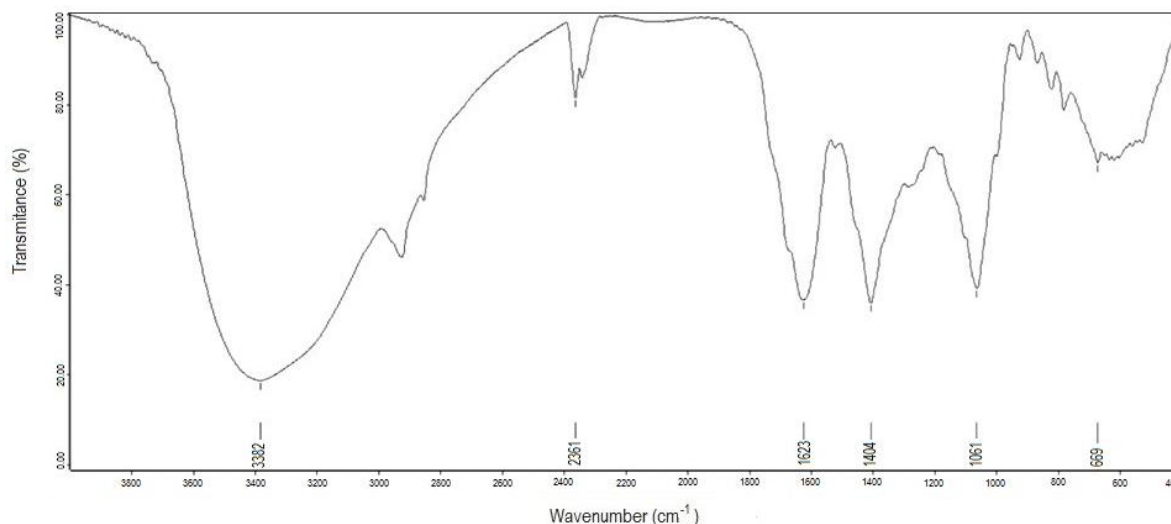


Figure 6. FTIR spectrum for pure *C. scolymus* extract.

On the other hand, a signal at 1623 cm^{-1} corresponds to the vibrations for the C=C link, characteristic for aromatic rings, and the signal at 1404 , 1061 and 669 cm^{-1} correspond to the vibrations of the methyl, $-\text{CH}_3$, group.

3.7 Gas Chromatography / Mass spectrometry (GC-MS)

The chromatogram for *C. scolymus* extract is given in Fig. 7, whereas the main compounds found are given in table 4.

Results show that the main compounds are: hexadecanoic and quinic acids were the two main compounds, followed by 2,3-dihidro-3,5-dihidroxi-6-metil(R)-4H-piran-4-one, which has been found in propolis, whereas ciclitol, some fatty acids with their esters, as well as stigmastherol and γ -sitosterol were found also. Structurally, organic corrosion inhibitors consist of polar and nonpolar ends. The polar end, which consists of heteroatoms such as oxygen, nitrogen, and sulphur, is usually adsorbed on the electrovalent metal surface. The heteroatoms usually have extra outer electrons to fill or share with the vacant d-orbital of the metal [7–10]. It has been shown [41] that the formation of a complex formed with Fe^{2+} ions and OH^- groups present in the extract is partially the responsible to give the corrosion protection to the metal.

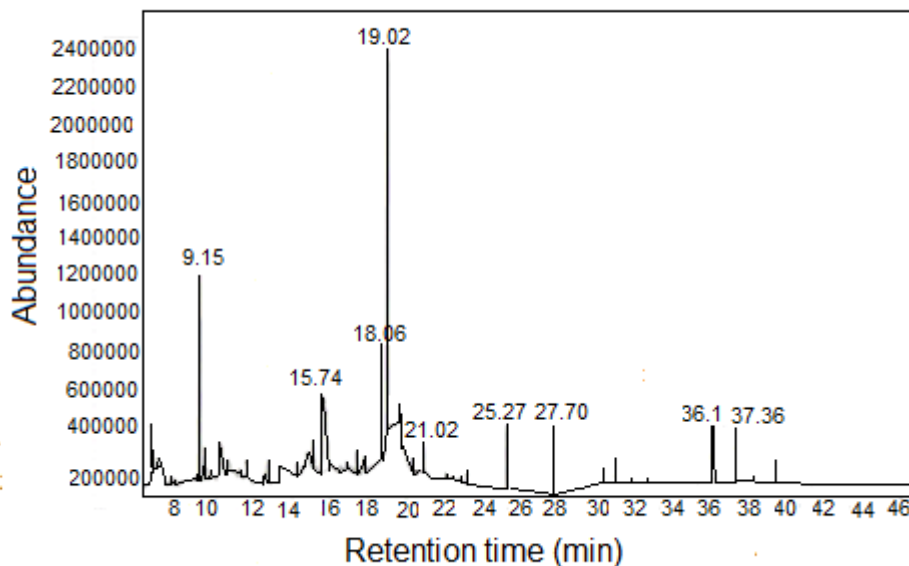
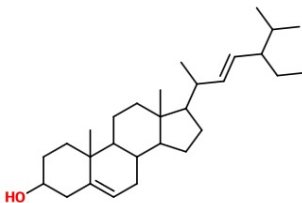
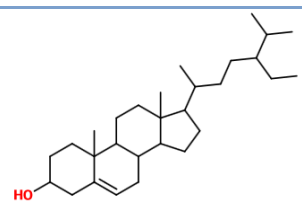


Figure 7. Gas Chromatography / Mass spectrometry spectrum for pure *C. scolymus* extract.

Table 4. Chemical compounds found in *C. scolymus* by using Gas Chromatography / Mass spectrometry.

Compound	t_r (min)	[M] ⁺	Chemical structure
2,3-dihidro-3,5-dihidroxi-6-metil(R)-4H-piran-4-on	9.15	144	
Quinic acid	15.74	174	
Methyl ester of hexadecanoic acid	18.66	270	
N-hexadecanoic acid	19.04	256	
Methyl ester of 9,12-octadecadienoic acid	20.31	294	
9, 12-octadienoic acid	20.66	280	
Octadecanoic acid	20.90	284	

Stigmasterol	36.11	412	
γ -sitosterol	37.36	414	

t_r = retention time, $[M]^+$ = Ion molecular mass.

It has been reported [22-24] that the most important compounds responsible for the antioxidant properties of *C. scolymus* are hexadecanoic and quinic acids, which contains OH^- groups within them. In this case, it seems that the OH^- group is the main responsible for the corrosion inhibition of *C. scolymus*. Additionally, in [42, 43] it was shown that the high inhibitive performance of this extract suggests a strong bonding of the *C. scolymus* derivatives on the metal surface due to presence of heteroatoms such as O, which have lone pairs and π -orbitals and vacant d -orbitals of 1018 steel, which block the active sites where corrosion takes [4,5, 18]. Therefore, bonding between inhibitor molecules onto carbon steel surface occurs through sharing electrons of the OH^- group present in the *C. scolymus* components of the extract and the d -orbitals of iron.

4. CONCLUSIONS

The possibility of using *C. scolymus* as a green corrosion inhibitor for 1018 steel in 0.5 M H_2SO_4 has been carried out. Results have shown that methanolic extract of *C. scolymus* petals is a good green corrosion inhibitor, with its efficiency increasing as the inhibitor concentration increased, reaching its highest value with the addition of 1000 ppm, but it decreases as the temperature increases. Polarization curves showed that the addition of *C. scolymus* decreases both the passive and the corrosion current density values. *C. scolymus* is physically adsorbed on the metal surface according to a Temkin isotherm type of adsorption of the green corrosion inhibitor which acts as a mixed type of inhibitor. SEM showed a layer formation of protective corrosion products film which is formed by iron ions and functional groups, mainly OH^- , present in the green corrosion inhibitor compounds such as hexadecanoic and quinic acids.

References

1. Y. Abed, Z. Arrar, A. Aouniti, B. Hammouti, S. Kertit, A. Mansri, *J. Chim. Phys.* 96 (1999)1347-1354.
2. R. Solmaz, *Corros. Sci.*, 81 (2014) 75-93.

3. M. Bouklah, A. Attayibat, S. Kertit, A. Ramdani, B. Hammouti, *Appl. Surf. Sci.* 242 (2005) 399-409.
4. M. Bouklah, N. Benchat, B. Hammouti, S. Kertit, *Mater. Let.* 60 (2006) 1901-1905.
5. D. Daoud, T. Douadi, S. Issaadi, S. Chafaa, *Corros. Sci.* 79 (2014) 50-65.
6. P. Muthukrishnan, B. Jeyaprabha, P. Prakash, *J. Mater. Eng. Perf.* 22 (2013) 3792-3803
7. B. Zhao, L.K. Zou, *Adv. Mater. Res.* 710 (2013) 41-49
8. A.S. Fouda, K. Shalabi, A.A. Idress, *Green Chem. Letters and Reviews*, 3-4 (2015) 17-29.
9. H. H. Abdel Rahman, S. M. Seleim , A. M.Hafez, A. A.Helmy, *Green Chemistry Letters and Reviews* 3-4 (2015) 88-94.
10. B. Ramezanzadeh, H. Vakili, R. Amini, *Appl. Surf. Sci.* 327 (2015) 174–181.
11. E. Kowsari, M. Payami, R. Amini, B. Ramezanzadeh, M. Javanbakht, *Appl. Surf. Sci.* 289 (2014) 478– 486.
12. A.M. Al-Turkustani, S.T. Arab, L.S.S. Al-Qarni, *J. Saudi Chem. Soc.* 15 (2011) 73–82.
13. Bingru Zhang, Chengjun He, Cheng Wang, Peidi Sun, Fengting Li, Yu Lin, *Corros. Sci.* 94 (2015) 6–20.
14. Xingwen Zheng, Shengtao Zhang, Wenpo Li, Min Gong, Linliang Yin *Corros. Sci.* 95 (2015) 168–179.
15. Ghulamullah khan, Kazi Md. Salim Newaz, Wan Jefrey Basirun, Hapipah Binti Mohd Ali, Fadhil, Lafta Faraj, Ghulam Mustafa Khan, *Int. J. Electrochem. Sci.* 10 (2015) 6120 – 6134.
16. S. Noyel Victoria, Rohith Prasad, R. Manivannan, *Int. J. Electrochem. Sci.* 10 (2015) 2220 – 2238.
17. M. R. Singh, *J. Mater. Environ. Sci.* 4 (2013) 117-126
18. K.K. Anupama, K. Ramya, K.M. Shainy, Abraham Joseph, *Mater. Chem. Phys.* in press, doi.org/10.1016/j.matchemphys.2015.09.013.
19. Gopal Ji, Shadma Anjum, Shanthi Sundaram, Rajiv Prakash, *Corros. Sci.* 90, (2015)107–117.
20. N. C. Ngobiri, E. E. Oguzie, Y. Li, L. Liu, N. C. Oforika, O. Akaranta, *Int. J. Corrosion*, 2015, 9 pages, doi.org/10.1155/2015/404139
21. Naoual El Hamdani, Rabiaa Fdil, Mustapha Tourabi, Charafeddine Jama, Fouad Bentiss, *Appl. Surf. Sci.* 357 (2015) 1294–1305.
22. Velayutham Rajeswari, Devarayan Kesavan, Mayakrishnan Gopiraman, Periasamy Viswanathamurthi, Kaliyaperumal Poonkuzhali, Thayumanavan Palvannan, *Appl. Surf. Sci.* 314 (2014) 537–545.
23. J. Bruneton, *Pharmacognosy Phytochemistry Medicinal Plants*; Lavoisier Publishing: Secaucus, NY, 1995; pp 218-219.
24. T. Adzet, M. Puigmacia, High-performance liquid chromatography of caffeoylquinic acid derivatives of *Cynara scolymus* L. leaves., *J. Chromatogr.* 348 (1985) 447-452.
25. L. I. Dranik, L. G. Dolganenko, J. Slapke, N.Thoma, *Rastit. Resur.* 32 (1996) 98-104.
26. E. A. Nichiforescu, *Plant Med. Phytother.*, 4 (1970) 56-62.
27. V. Martino, N. Caffini, J. D. Phillipson, A. Lappa, A; Tchernitchin, G. Ferraro, S. Debenedelti, H. Schilcher, C. Acevedo, *Acta Hort.*, 501 (1999) 111-114.
28. B. Mcdougall, P. J. King, B. W. Wu, Z. Hostomsky, G. Manfred, , W. E. Robinsaon , *Antimicrob. Agents Chemother.* 42 (1998) 140-146.
29. K. Kraft, *Phytomedicine*, 4 (1997) 369-378.
30. J. E. Brown, C. A. Rice-Evans, *Free Radical Res.*, 29 (1998) 247-255.
31. R. Gibhardt, *Toxicol. Appl. Pharmacol.*, 144 (1997) 279-286.
32. R. L. Horst, T. A. Reinhardt, J. R. Russel, J. L. Napoli, *Arch. Biochem. Biophys.*, 231(1984) 67-71.
33. K. S. Bora, *Pharm. Biol.*, 49 (2011) 211-220.
34. R. Fuchs-Godec, V. Dolecek, *Colloids Surf. A.* 244 (2004) 73–76.
35. I. Kowalska, A. Stochmal, I. Kapusta, B. Janda, C.Pizza, S. Piacente, W. Oleszek, *J. Agr. Food Chem.*, 55 (2007), 2645-2652.
36. A. Stochmal, W.Oleszek, *J. Food Agric. Environ.*, 5 (2007) 170-174.

37. A. Popova, E. Sokolova, S. Raicheva and M. Christov, *Corros. Sci.*, 45 (2003) 33-59.
38. M. Özcan, İ. Dehri, M. Erbil, *Appl. Surf. Sci.*, 236 (2004) 155–164.
39. R. Solmaz, G. Kardas, M. Culha, B. Yazıcı, M. Erbil, *Electrochim. Acta*, 53 (2008) 5941–5952.
40. F. Bontiss, M. Lagrence, M. Traisnel, *Corrosion*, 56 (2000), 733-742.
41. Y. Okada, K. Tanaka, E. Sato, H. Okajima, *Org. Biomol. Chem.*, 4 (2006), 4113-4117.
42. R. Solmaz, E.A. Sahin, A. Doner, G. Kardas, *Corros. Sci.*, 53 (2011), 3231–3240.
43. R. Hilal, A. A. Abdel Khalegh, S. A. K. Elroby, *Int. J. Quant. Chem.*, 103 (2005) 332–343.

© 2016 The Authors. Published by ESG (www.electrochemsci.org). This article is an open access article distributed under the terms and conditions of the Creative Commons Attribution license (<http://creativecommons.org/licenses/by/4.0/>).